CONF-810618--1

LA-UR-81-534

TITLE: EXPERIMENTALLY DETERMINED ROCK-FLUID INTERACTIONS APPLICABLE TO A NATURAL HOT-DRY-ROCK GEOTHERMAL SYSTEM

AUTHOR(S): R. W. Charles, C. O. Grigsby, C. E. Holley, Jr., J. W. Tester, and L. A. Blatz

SUBMITTED TO: Metallurgical Society of AIME
For publication in the conference proceedings from the 1979, 1980, and 1981 meetings, as a Symposium Volume, entitled "Process Mineralogy in Extractive Metallurgy," Summer, 1981.

University of California

LOS ALAMOS SCIENTIFIC LABORATORY
Post Office Box 1663 Los Alamos, New Mexico 87545
An Affirmative Action/Equal Opportunity Employer

Form No. 836 R3
St. No. 2629
12/78

UNITED STATES
DEPARTMENT OF ENERGY
CONTRACT W-7405-ENG. 36

DISCLAIMER

EXPERIMENTALLY DETERMINED ROCK-FLUID INTERACTIONS APPLICABLE TO A NATURAL HOT DRY ROCK GEOTHERMAL SYSTEM

R. W. Charles, C. O. Grigsby, C. E. Holley, Jr.,
J. W. Tester,* and L. A. Blatz
Los Alamos National Laboratory, Los Alamos, New Mexico 87545

*Current address: Department of Chemical Engineering
Massachusetts Institute of Technology, Cambridge, MA 02139

Summary

The Los Alamos National Laboratory, under the sponsorship of the U.S. Department of Energy, is involved with laboratory and field experiments to assist in development of the Hot Dry Rock concept of geothermal energy. The field program consists of experiments in which hot rock of low permeability is hydraulically fractured between two wellbores. Water is circulated from one well to the other through the fractured hot rock. Our field experiments are designed to test reservoir engineering parameters such as heat-extraction rates, water-loss rates, flow characteristics including impedance and buoyancy, seismic activity, and fluid chemistry. Laboratory experiments were designed to provide information on the mineral-water reactivity encountered during the field program. Two experimental circulation systems tested the rates of dissolution and alteration during dynamic flow. Solubility of rock in agitated systems was studied. Moreover, pure minerals, samples of the granodiorite from the actual reservoir, and Tijeras Canyon granite have been reacted with distilled water and various solutions of NaCl, NaOH, and Na_2CO_3. The results of these experimental systems are compared to the observations made in field experiments done within the hot dry rock reservoir at a depth of approximately 3 km where the initial rock temperature was 150 to 200°C.

Table I - Characteristics of the Phase 1 Fenton Hill Hot Dry Rock System

Reservoirs

depths	2.5-3 km
initial rock temperatures	180-200°C
major rock type*	biotite granodiorite
density	2700 kg/m^3
specific heat	1000 J/kgK
permeability (matrix)*	10^{-18} to 10^{-20} m^2 (1 to 10^{-2} μ darcy)
porosity (matrix)*	$\sim 10^{-3}$
permeability (*in situ*)	10^{-15} to 10^{-17} m^2
porosity (*in situ*)	10^{-3} 10^{-5}
thermal conductivity	2.8 W/mK
thermal diffusivity	10^{-6} m^2/s
p-wave velocity V_p	5.9 km/s
V_p/V_s	1.7

Wellbores

Injection well (EE-1) - - - 3.07 km total depth cased with 7 5/8-in. and 8 5/8-in. steel casing to 2.95 km main injection zone at 2750 m behind casing.

Production well (GT-2B) - - - 2.70 km total depth cased with 7 5/8-in. steel casing to 2.60 km main production zone at 2660 m in open hole.

Surface Plant

Circulation pumps - - - Multi-stage centrifugal ΔP = 100 bar

Heat exchanger - - - - Forced draft-air cooled carbon steel tubes with aluminum fins.

*Determined from cores.

Introduction

Under sponsorship of the U.S. Department of Energy, Los Alamos National Laboratory is conducting field and laboratory experiments to develop a means of extracting energy from deep, impermeable hot rock. The concept -- known as hot dry rock (HDR) geothermal energy -- involves creation of a heat transfer surface by hydraulic fracturing of hot rock between two wells.

In a commercial-sized system, energy would be removed by circulating pressurized water over 1 to 2 km^2 of rock surface with initial temperatures from 200 to 300°C at depths of 4-5 km (1,12,13). Continuous rapid circulation of water over hot rock surfaces is required to ensure economically acceptable production rates. Large heat-extraction surface areas are needed because of the inherently low thermal conductivity of rock, which quickly controls the rate at which heat is transferred to the fluid contained within the fracture.

This rather unique set of operating conditions and reservoir characteristics results in a different set of crystallization/dissolution problems than those normally encountered in natural hydrothermal environments. The kinetics and equilibria associated with in situ granite-water interactions are important in determining how the fluid and rock composition of the system will vary over the 20-40 year lifetime of a typical hot dry rock (HDR) power plant. The extent of this chemical interaction can have profound effects on the performance of the reservoir and the surface plant. For example, pressure drop and fluid circulation patterns within the fracture as well as fluid permeation losses will be influenced by local chemical dissolution and reprecipitation reactions occurring on and near the fracture faces. Dissolved material, particularly silica and carbonates, may deposit on heat exchange surfaces because of the large pressure and temperature differences experienced as fluid is heated within the reservoir and cooled in the surface heat exchange system.

Our current program includes laboratory and theoretical studies directed toward understanding geochemical alteration, morphological changes, dissolution kinetics, solubility, and scale deposition in the granite-water system. These laboratory studies proved useful in predicting as well as interpreting the performance of the field system. The first two sections of this paper discuss experimental aspects of the program, the third section deals primarily with the geochemical behavior of the field reservoir during 75 days of closed loop circulation. The general characteristics and properties of the system at the Fenton Hill site are listed in Table 1.

This paper is a summary of the salient features of our work. Interested readers should consult references 1, 12, 13, 14, and 15 for details.

Rock - Water Interactions

Introduction

Rock-water reactions are critical to the long-term life of a HDR reservoir. Static experiments, although important, only determine the equilibrium phase assemblage which will be compatible in the rock reservoir for a given set of physical conditions. Dynamic (circulatory) systems have been built which model the pressure and temperature conditions encountered

in the HDR reservoir. The phase relations of the biotite granodiorite reservoir rock in contact with a circulating dilute aqueous solution have direct application to the field experiments. Physical and chemical changes occurring in the experimental rock samples indicate how the actual rock reservoir may be expected to behave. Removal of material may be a problem, and deposition of material may constrict the circulation loop below or above ground. Important questions are: How are the original minerals attacked -- along grain boundaries, fractures, or compositional zones? Which minerals are attacked? Where do secondary phases grow and why?

Experimental System

The experimental system (Figure 1) consists of a loop in which the aqueous solution moves slowly in sequence through a heated chamber containing rock samples, through a cooling column, through a circulating pump, and then back to the heated chamber. Pressure within the system is maintained by a second pump. The temperature of the sample chamber is controlled by a tube furnace while the temperature of the loop between the sample chamber and cooling column is maintained by heating tapes. The cooling column has a central core of platinum gauze on a tantalum rod for collection of scale. All heated portions of the system are gold-plated to prevent spurious reactions. During an experiment, circulation is maintained continuously at 2.5 cm^3/min. for the 560 cm^3 system during the work week, however the flow is stopped at temperature and pressure during the weekend.

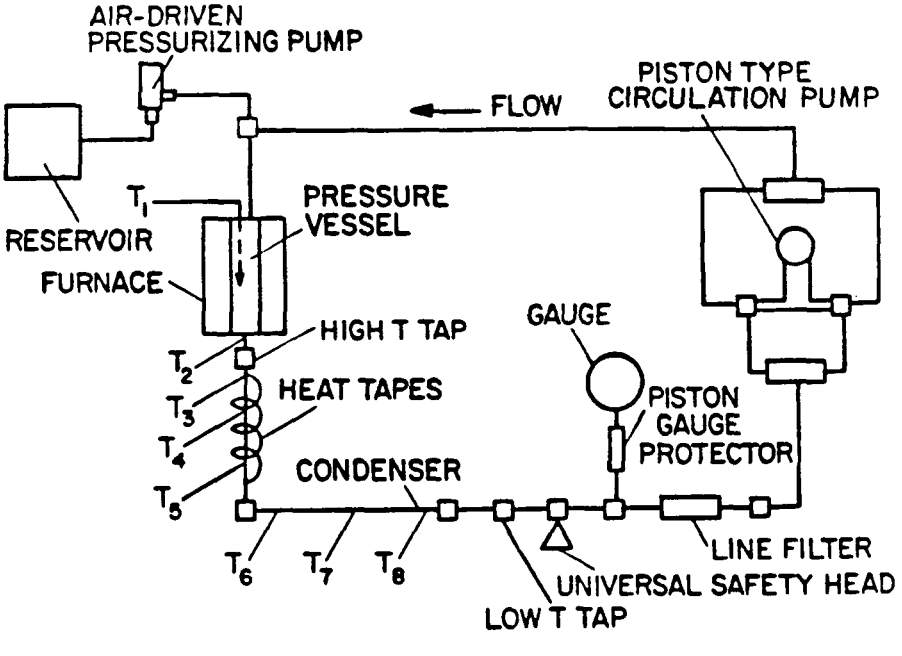

Fig. 1 - Fixed Temperature Circulation System.
Note: T_{1-3} are thermocouples.

Eight polished rock disks 3 mm thick and 19 mm in diameter are mounted vertically on a carousel made of tantalum, placing the rock disks at the center of the vertically mounted 500 mℓ pressure vessel.

Some results presented here in detail are from an experiment reacting biotite granodiorite with distilled water at 200°C and 1/3 kbar pressure for a total time of 9 mo. Disks 1 through 3 were removed at 1, 2, and 4 mo. The remainder were removed at 9 mo. Solutions were sampled at 29, 53, 213, 817, 1372, 3147, and 6579 h. Reacted rock surfaces were examined by scanning electron microscopy and electron microprobe. Solutions were analyzed by atomic absorption. This experiment is supplemented by others done under different physical conditions.

Rock Alteration

Introduction. Initial modal analysis of the rock is shown in Table II. Fourteen phases have been identified. Kspar (var. microcline, Or_{93}) is relatively fresh. Plagioclase shows a bimodal composition. The albite-rich rims (Ab_{89}) surround a core of oligoclase (Ab_{74}). Biotite is commonly chloritized. Original biotite always shows a K deficiency and is too aluminous to be on the annite-phlogopite join. Sphene, apatite, magnetite, and zircon complete the primary mineral phases. In addition to chlorite, metamorphic alteration has produced epidote, sericite, calcite, and a trace of prehnite.

The initial surface is smooth, but shows some natural fractures filled by veins of quartz and calcite.

After 9 mo. reaction, the quartz and microcline are etched. A filmy white material, compositionally the zeolite phillipsite, almost entirely covers the plagioclase. Some plagioclase exhibits etching along twin planes. Much of the plagioclase is pock-marked. Biotite and the minor primary phases remain resistant. Relative reactivity is: quartz > plagioclase > microcline > mafics and trace phases. The natural hydrothermal alterations (sericite, epidote, prehnite, and chlorite) show resistance to the distilled water leach. Veins originally containing calcite were deeply

Table II - Biotite Granodiorite Modal Analysis

Phase	Percent
Microcline	15
Plagioclase	40
Quartz	30
Biotite and Chlorite	7
Magnetite	1
Epidote	1
Sphene	2
Calcite	2
Apatite	2
Zircon	tr.
Sericite	tr.
Sulfide	tr.
Prehnite	tr.

attacked. The other rock disks removed at 1, 2, and 4 mo. show similar alteration, although less advanced.

The rock disks underwent a net weight loss: 1 mo.-1.3%, 2 mo.-1.8%, 4 mo.-3.4%, and 9 mo. (ave. of five)-5.4%.

Chemical Alteration. As mentioned, the original phases ranged widely in reactivity, as shown by their change in morphology. Table III presents compositional data.

Quartz was congruently dissolved. Microcline also showed essentially congruent dissolution, whereas plagioclase reacted with solution in less than a month (817 h) to yield experimental secondary overgrowths. Analyses of plagioclase grouped into four categories: plagioclase, naturally altered plagioclase, and two experimentally grown alterations, phillipsite and possible laumontite (see Table IV).

Biotites show some chemical change. Between 4 and 9 mo. crusty chromium rich overgrowths appear on the biotite in addition to loss of potassium. Excess chromium only appears from biotite. The biotite appears to be undergoing replacement of Mg by Cr. Chlorite does not show this effect. Chlorite remains resistant throughout the experiment. Epidote and sericite are also resistant. Sericite is considerably more silicic than muscovite. Other phases are resistant.

Table III - Major Phase Composition Before and After Reaction

Phase	Composition
Microcline (fresh)	$K_{0.93}Na_{0.07}Al_{1.02}Si_{2.98}O_8$
(9 mo.)	$K_{0.94}Na_{0.04}Al_{1.03}Si_{2.98}O_8$
Plagioclase (fresh)	Core: $Na_{0.74}K_{0.01}Ca_{0.26}Al_{1.28}Si_{2.72}O_8$
	Rim: $Na_{0.89}K_{0.02}Ca_{0.09}Al_{1.13}Si_{2.87}O_8$
(9 mo.)	Plagioclase rarely found. Substrate covered by secondary alterations. All analyses on reacted plagioclase are presented in Table V.
Biotote (fresh)	$K_{0.88}Mg_{1.37}Fe_{1.21}Mn_{0.04}Ti_{0.09}Al_{1.41}Si_{2.81}O_{10}(OH)_2$*
(9 mo.)	$K_{0.40}Ca_{0.01}Mg_{0.95}Fe_{1.20}Cr_{0.22}Ti_{0.10}Mn_{0.04}Al_{1.52}Si_{2.86}O_{10}(OH)_2$
Chlorite (fresh)	$Mg_{2.50}Al_{2.49}Fe_{2.18}Mn_{0.08}Si_{2.73}O_{10}(OH)_8$
(9 mo.)	$K_{0.02}Ca_{0.05}Mg_{2.17}Al_{2.39}Fe_{1.67}Ti_{0.03}Mn_{0.05}Si_{3.06}O_{10}(OH)_8$
Epidote (fresh)	$Ca_{1.99}Fe_{0.77}Al_{2.24}Si_{3.11}O_{12}(OH)$
(9 mo.)	$Ca_{1.93}Fe_{0.77}Al_{2.21}Si_{3.14}O_{12}(OH)$
Sphene (fresh)	$Ca_{1.00}Al_{0.09}Fe_{0.06}Ti_{0.87}Si_{1.03}O_5$
(9 mo.)	$Ca_{0.96}Al_{0.19}Fe_{0.07}Ti_{0.76}Si_{1.06}O_5$
Sericite (fresh)	$K_{0.89}Na_{0.03}Mg_{0.13}Fe_{0.24}Al_{2.60}Si_{3.17}O_{10}(OH)_2$
(9 mo.)	$K_{0.90}Na_{0.02}Mg_{0.08}Fe_{0.18}Al_{2.61}Si_{3.10}O_{10}(OH)_2$
Prehnite (fresh)	$Ca_{1.92}Al_{1.99}Si_{3.02}O_{10}(OH)_2$

*All Fe calculated as 2+ with the exception of epidote.

Table IV - Secondary Phases Grown on Plagioclase

Phillipsite is reduced to 16(O) and laumontite plus plagioclase mixture is reduced to 8(O).

Phillipsite

817h	$Ca_{0.79}Na_{0.23}K_{0.70}Mn_{0.01}Mg_{0.09}Fe_{0.11}Al_{3.73}Si_{4.53}O_{16}\cdot H_2O$
1632h	$Ca_{0.96}Na_{0.17}K_{0.62}Mn_{0.00}Mg_{0.03}Fe_{0.05}Al_{3.80}Si_{4.42}O_{16}\cdot H_2O$
3147h	$Ca_{0.85}Na_{0.13}K_{0.73}Mn_{0.00}Mg_{0.06}Fe_{0.11}Al_{3.76}Si_{4.36}O_{16}\cdot H_2O$
6579h	$Ca_{0.93}Na_{0.11}K_{0.73}Mn_{0.03}Mg_{0.05}Fe_{0.13}Al_{3.74}Si_{4.38}O_{16}\cdot H_2O$

Laumontite plus Plagioclase Substrate

817h	$Ca_{0.39}Na_{0.48}K_{0.05}Al_{1.42}Si_{2.58}O_8$
1632h	$Ca_{0.31}Na_{0.53}K_{0.03}Al_{1.39}Si_{2.64}O_8$
3147h	$Ca_{0.38}Na_{0.55}K_{0.00}Al_{1.40}Si_{2.60}O_8$
6579h	$Ca_{0.41}Na_{0.47}K_{0.03}Al_{1.43}Si_{2.57}O_8$

Scaling. Although infrequent, scaling was observed. Screen samples showed it to be primarily silicic. This contrasts with a similar experiment done at 300°C where alpha quartz, amorphous silica, Ca-Si hydrate, and wollastonite were observed.

Solution Composition. Solution compositions (analysed by atomic absorption) are presented in Table V. Silica reached a steady state of about 170 ppm after about 2 mo. All other cations, with the exception of Na, leveled off after a few days. Sodium did not reach a steady state until about 4 mo. Total solution burden reached 190 - 200 ppm.

Discussion

Mass Balance. Initially, the eight rock disks weighed a total of 22.9808 g. Final cumulative weight is 22.0099 g (after drying) for a net loss of 0.9709 g, or 4.2%. If the weight loss were calculated as silica alone, the volume loss is 0.37 cm^3 or 4.3% of the total volume of 8.54 cm^3.

Rock density was determined by two methods. First, the regular disk shape facilitated volume calculation (8.54 cm^3). This yields a density of 2.69 g/cm^3. Second, the density was estimated by the mineralogy and modal analysis. Densities of minerals were taken from Robie et al.(11). Biotite was approximated by $annite_{33}phlogopite_{66}$ and epidote was calculated as $zoisite_{66}pistacite_{33}$. Calculated density by this method is 2.73 g/cm^3.

Both methods have their shortcomings. The first ignores void space, which yields a low density. The second assumes no void space, which will yield a high density. Also, this method has a random error due to approximations necessary to calculate the densities of the solid solution minerals. Both methods should bracket the real density: about 2.71 ± 0.02 g/cm^3.

Table V - Solution Analyses (ppm ± 5%)

Time	SiO_2	Al	Fe	Ca	Na	K	Total
29h	79	2.1	0.20	3.4	8.6	5.8	101
53	67	4.0	0.40	3.2	7.9	4.5	88
213	92	4.1	0.60	4.2	8.8	5.0	115
817	124	2.4	0.30	2.4	9.5	4.1	143
1372	153	n.d.	n.d.	n.d.	n.d.	n.d.	---
3147	173	4.0	0.70	2.4	16.2	5.0	201
6579	162	4.2	0.70	1.4	17.1	3.5	190

For a weight loss of 0.9709 g, if the rock reacted congruently, one would expect a volume loss of 0.36 cm^3 (4.2%), which compares favorably with the assumption of only quartz loss (0.37 cm^3).

A mean solution burden of 190 ppm was measured at the conclusion of the experiment. For a system volume of 560 cm^3, this accounts for 11% of the weight loss. About 500 mℓ were removed (and replaced with distilled water) for sampling. This accounts for about 10% more material. The remaining 79% occurs as small deposits of scale which cannot be weighed directly.

Weight Loss. The weight loss data were fitted with a power function (see Fig. 2):

4 point fit: $wt.\%loss = 0.0106\ t^{0.7009}$, $r^2 = 0.99$.

where t = time in hours, and r^2 = correlation coefficient.

Because surface damage due to sample preparation may make the first weight loss point somewhat high, the data were reduced again using only the last three points:

3 point fit: $wt.\%loss = 0.0056\ t^{0.7008}$, $r^2 = 0.99$.

This rate function is controlled primarily by quartz dissolution. Once quartz is entirely removed, different reactions buffered by feldspar dissolution will change the kinetics of dissolution.

Geochemical Thermometry. The silica geothermometer of Morey et al.(10) and the Na-Ca-K geothermometer of Fournier and Truesdell(5), can be used in the experimental and natural systems. For the experimental system, T(quartz at 1 kbar) = 148°C, T (quartz along the vapor pressure curve) = 167°C, and T (Na-Ca-K) = 203°C. The known temperature for the laboratory experiment was 200 ± 5°C.

Early fluid samples taken from the Fenton Hill system (before the 75 day experiment) yield Na-Ca-K temperatures of 198°C vs. a 197°C original well temperature, while the silica thermometer yields a temperature of 188°C.

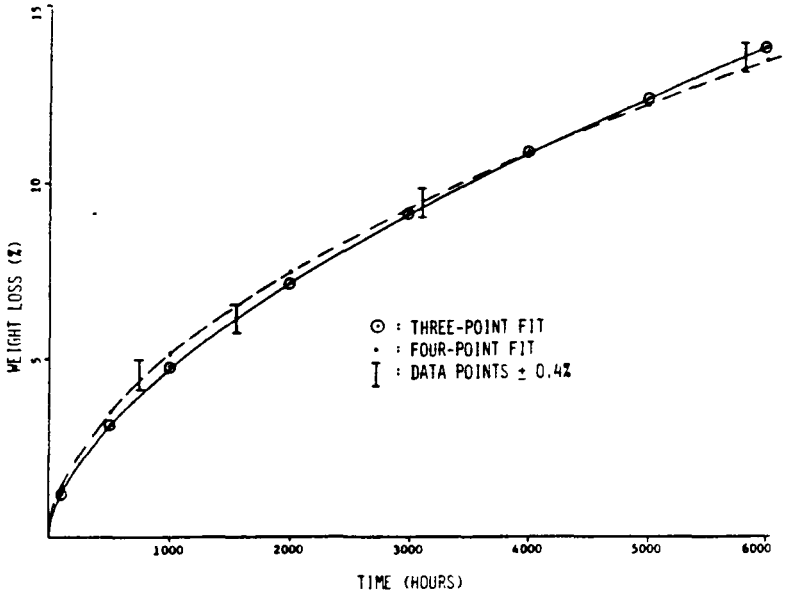

Fig. 2 - Weight Loss (%) vs. Run Duration (h).

More detailed examination of the data presented here, as well as under different experimental conditions, are presented in Charles (2 and 3).

Dissolution Kinetics and Solubility

Experimental Apparatus and Procedures

Small Agitated Vessels. Small stainless vessels with teflon cup liners similar to Parr Instrument Company's vessel (Bulletin 4745) were used for the study of the solubility of amorphous silica and for some of the kinetic studies. Closure was by means of a steel spring which was compressed when the lid of the bomb was screwed onto the body pressing the cap of the cup against its body for a teflon-to-teflon seal. The vessels were agitated gently in an oven on a rocking platform. For rapid heating to temperature, heat tapes were wrapped around the bombs to provide heat additional to that provided by the oven.

For an experiment, one gram of silica or granite and 15 mℓ of water or solution were placed in the teflon cup, the equipment assembled, and the heating begun. At the end of the heating period, the bomb was quenched in liquid nitrogen but removed before the contents had frozen and warmed to room temperature with water. Samples were then taken for pH measurements and silica analyses. Monomeric silica was determined spectrophotometrically using the ammonium molybdate method, and total silica was measured by atomic absorption.

Model Geothermal Test Loop. The model geothermal test loop is designed to operate at temperatures up to 300 ℃ and pressures up to 0.1 kbar (1500 psi) with flow rates of 15 to 151 ℓ/h. The system consists of a

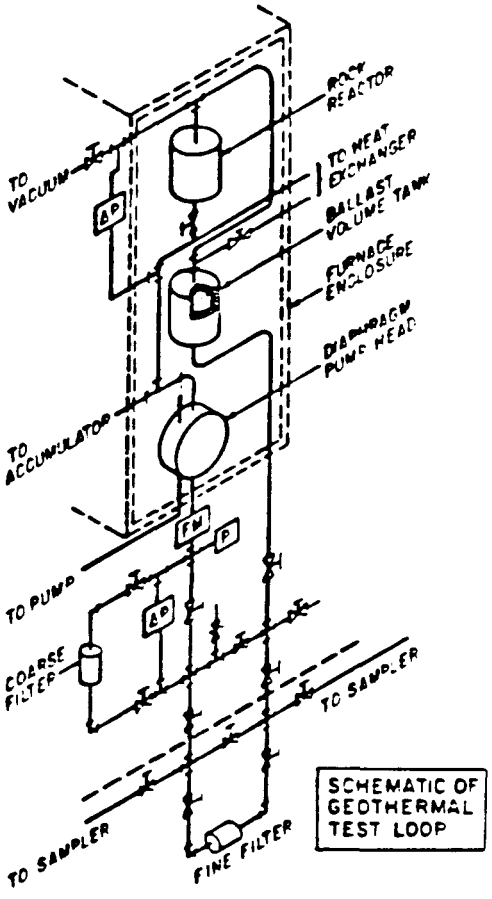

Fig. 3 - Model Geothermal Test Loop.

5-ℓ rock reactor, a 10-ℓ ballast volume, a diaphragm pumping head located in an oven, and associated equipment (see Figure 3). For corrosion resistance nearly all parts are made of commercially pure titanium. The rock reactor has a titanium flow distributor, mounted a couple of centimeters above the bottom to even out the upward flow of solution through the rock particles and minimize channeling. A 65-μm filter protects the pump from large rock particles. The sampler is of the flow-through type. During use, the sample is attached to the system and evacuated. The flow is then diverted through the sampler for a few minutes before the sample is taken. The accumulator damps out the pumping pulses, provides a space into which the water can expand as it is heated, and replenishes water removed by sampling. The pressure in the accumulator is set at slightly higher than water vapor pressure at the temperature of the experiment to suppress the vapor phase. At the start of an experiment, the flow bypasses the rock reactor until the operating temperature is reached, which takes about 2 h. The zero time is taken as the time when temperature has been reached and the flow is switched into the rock reactor.

Results

Solubility of Amorphous Silica. These experiments were done in small bombs at 200°C using Baker's ultrex SiO_2 and distilled water. Various equilibration times were used, and a steady state value of monomeric silica of 995 ± 10 ppm was reached in 2 d. However, when the same silica sample was treated with successive amounts of fresh distilled water the apparent solubility in 2 d decreased successively to about 800 ppm, 450 ppm, and 350 ppm. The lengths of time were then increased and the values obtained were, after 4 d about 400 ppm, after 8 d about 600 ppm, and after 16 d about 700 ppm. There was considerable variation among duplicate runs.

Fresh silica particles were then examined under the scanning electron microscope. Each particle was covered with very many small particles, less than a micron in size. Probably these very small particles give the high rate of dissolution and high apparent solubility observed initially.

Interaction of Fenton Hill Granodiorite with Aqueous Sodium Carbonate and Aqueous Sodium Hydroxide. Dissolution rate and solubility data for reactions between granodiorite cuttings and solution of NaOH and Na_2CO_3 were obtained in a series of agitated vessel experiments. This information was used in the design and interpretation of a leaching experiment conducted at Fenton Hill(13).

Experiments were done with 0.1 N, 0.3 N, 1.0 N, and 3.0 N aqueous sodium carbonate and with 0.5 N, 0.1 N, and 1.0 N aqueous sodium hydroxide for times of 2, 4, 7, 12, 24, 48, and 96 h. The silica contents and the pH of the resulting solutions were measured.

The results are shown in Figures 4 and 5.

Interaction of Tijeras Canyon Granite with Water. Experiments to investigate the effects of flow rate on the build-up of silica in solution were done in the small geothermal test loop on Tijeras Canyon granite, which is similar in composition to the Fenton Hill granodiorite.

These experiments were done at flow rates of 0.4 and 2.2 ℓ/min. and temperatures of 175°C, 200°C, and 225°C. The results are shown in Figure 6.

Discussion

Solubility of Amorphous Silica. The apparent solubility of fresh amorphous silica in teflon at 200°C of about 995 ± 10 ppm is somewhat higher than the 934 ± 50 ppm given by Walker (8) as a composite value from the work of a number of investigators. However, because of the presence of the very fine particles on the surface of the silica and the slow rate of approach to equilibrium, this solubility value must be considered approximate.

Interaction of Fenton Hill Granite with Aqueous Sodium Carbonate and Aqueous Sodium Hydroxide. The results of these experiments are qualitatively as expected. The dissolved silica increases rapidly with time initially and approaches asymptotically, for each concentration of solvent, a value characteristic of that concentration. Both the initial rate and the final value are higher for more concentrated solvents.

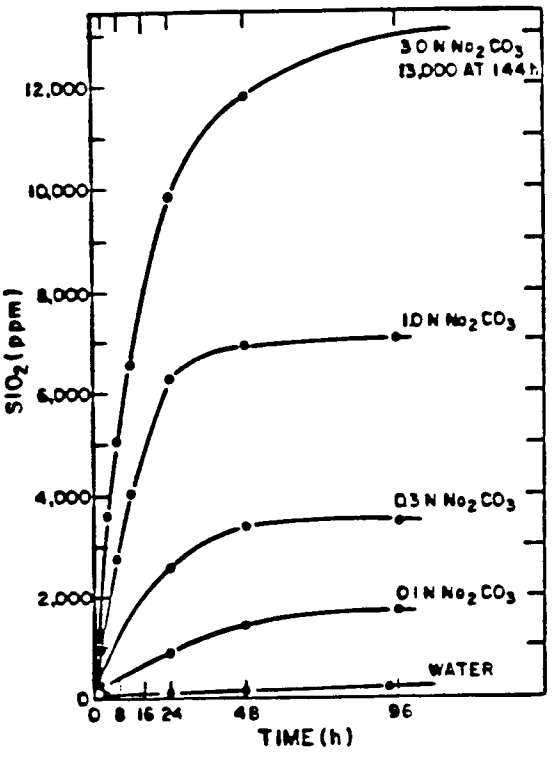

Fig. 4 - Solubility of Silica for Fenton Hill Granodiorite vs. Time at the Sodium Carbonate Concentration Indicated.

If the initial rates are plotted against the saturation values for the corresponding concentrations, a straight line results for both sodium carbonate and sodium hydroxide. This is consistent with a rate law which says that the rate of dissolution of silica from the granite is equal to some constant times the difference between the saturation value and the existing value of the soluble silica:

$$\frac{d(SiO_2)}{dt} = ak\left[[SiO_2]_{Sat} - [SiO_2]\right] \qquad (1)$$

a = rock area to fluid volume parameter
k = rate constant = f (T, flow conditions, other parameters).

On integration this becomes:

$$\ln\left\{\frac{[SiO_2]_{Sat} - [SiO_2]}{[SiO_2]_{Sat}}\right\} = -akt \quad . \qquad (2)$$

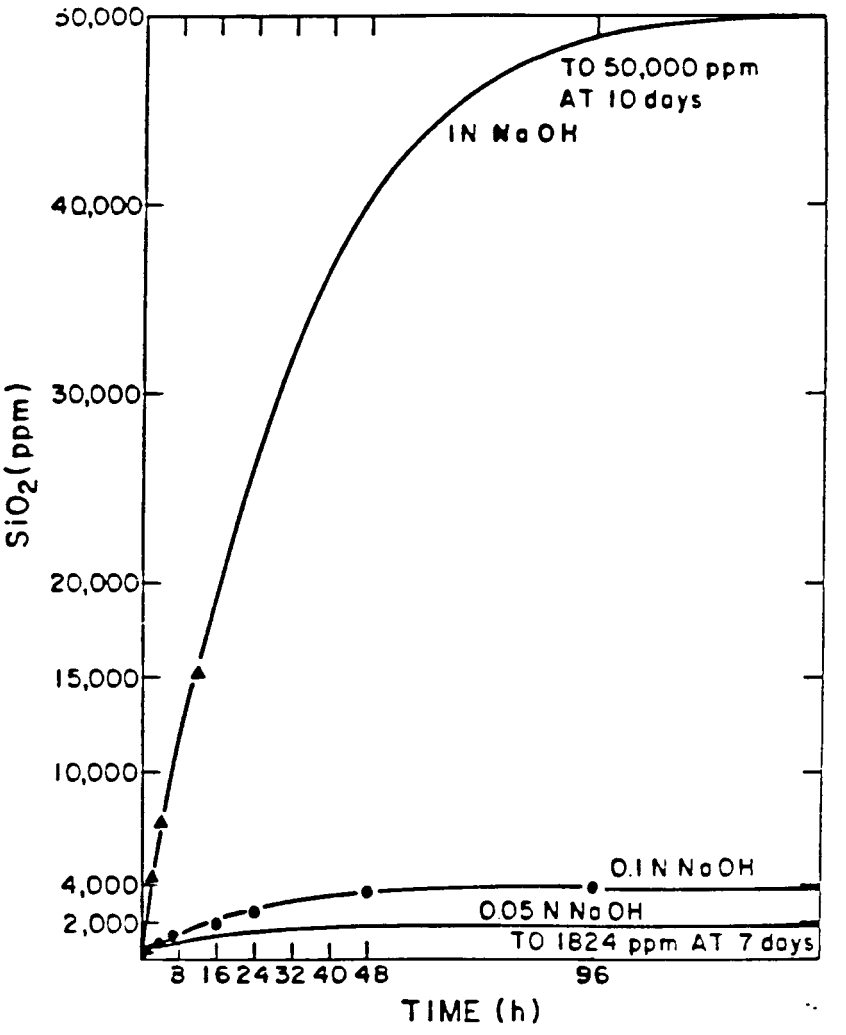

Fig. 5 - Solubility of Silica from Fenton Hill Granodiorite vs. Time at the Sodium Hydroxide Concentrations Indicated.

This rate law is successful in correlating the data as seen in Figures 7 and 8.

From the pH measurements it is possible, with a few assumptions, to calculate the number of hydroxyl ions (n) which have reacted with a silica molecule:

$$SiO_2 + nOH^- = H_nSiO_{2+n}^{-n}$$

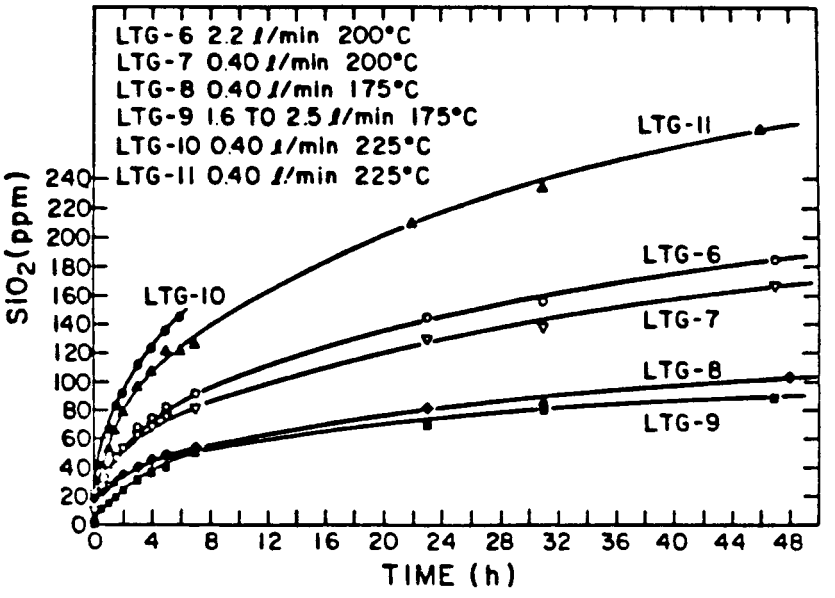

Fig. 6 - Silica Buildup in Model Geothermal Loop using Tijeras Canyon Granite and Distilled Water.

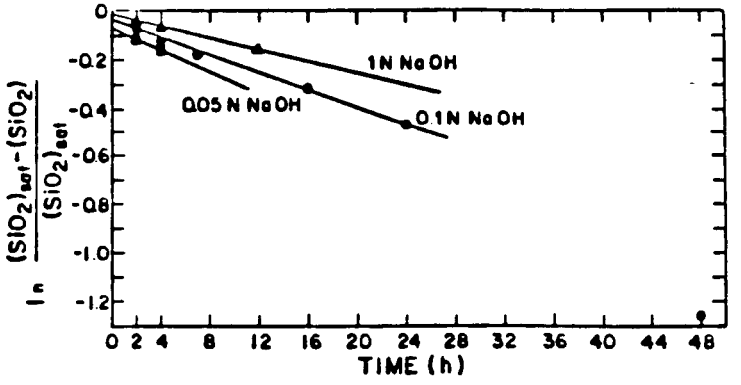

Fig. 7 - Integrated Rate Equation Compared with the Sodium Hydroxide Data.

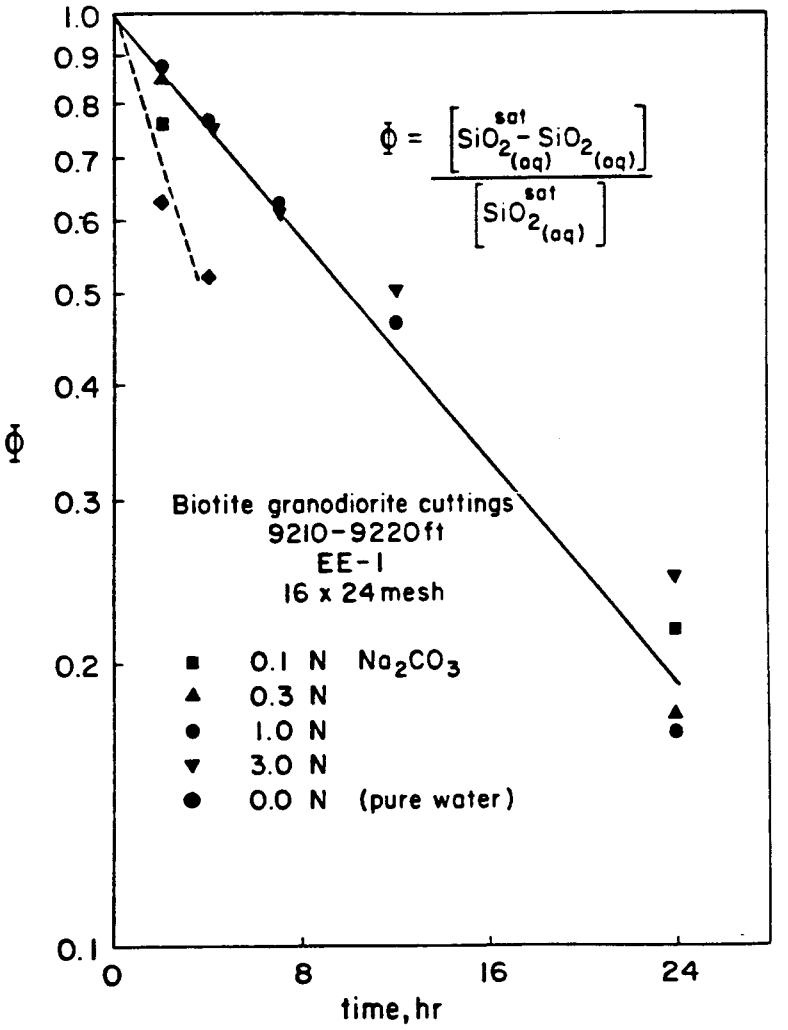

Fig. 8 - Integrated Rate Equation Compared with Sodium Carbonate Data.

and thus suggests a form for the aqueous species. For the sodium hydroxide solutions this is fairly straightforward and n is 1 or a little more than 1 (see Table VI) as expected from the ionization constant of silicic acid. For the sodium carbonate solutions, because of the hydrolysis reaction of the carbonate ion, additional measurements were needed on the pH of solutions with various carbonate ion/bicarbonate ion ratios. The value of n then calculated is 1 or a little less than 1 (see Table VII). However, because of the increased number of assumptions involved in this latter calculation, the agreement is reasonable.

These measurements and calculations were made on solutions cooled to room temperature and may not duplicate the conditions at 200°C, the temperature of the experiments.

Table VI - Calculated Values of n (Eq. 3) for NaOH Solution

	0.05 N NaOH	0.10 N NaOH	1.0 N NaOH
2 hours	1.25	---	1.76
4 hours	1.17	---	1.37
7 hours	---	---	---
12 hours	---	---	1.22
24 hours	---	1.41	1.32
48 hours	---	1.37	1.21
96 hours	---	1.34	---
7 days	1.24	---	1.03
10 days	---	1.20	1.05

Table VII - Calculated Values for n (Eq. 3) for Na_2CO_3 Solution

	Calculated values of n			
	0.1 N Na_2CO_3	0.3 N Na_2CO_3	1.0 N Na_2CO_3	3.0 N Na_2CO_3
2 hours	0.27	1.42	0.87	---
4 hours	---	---	0.87	0.85
7 hours	---	---	0.85	0.86
12 hours	---	---	---	0.78
24 hours	1.08	0.62	---	0.89
48 hours	0.83	0.57	---	0.51
96 hours	0.81	0.71	---	0.46

Interaction of Tijeras Canyon Granite with Water. At lower temperatures there should be no effect of flow rate on dissolution because the rate-limiting step would be a surface-controlled hydrolysis reaction. At higher temperatures, the surface reaction rate may be fast enough for diffusional transport from the rock surface to the bulk solution to be limiting. As is seen in Figure 6, at 200°C the slower flow rate gave a slower rate of dissolution, but at 175°C the effect was reversed. The runs are numbered in the order in which they were done, and at a given temperature, the second run gives a slower rate of dissolution than the first. It is probably the order in which the experiments were done and not the flow rate which is causing the effect. The fresh rock has many fine particles, corners, and edges, which have a higher reactivity than the bulk rock. As these are dissolved away, the apparent rate of dissolution decreases which is similar to the results of the experiments in the small vessels.

Field Experiments

Flow through the fracture system during a 75-day circulation test was distributed between several injection zones in well EE-1 and production zones in well GT-2B as shown in Fig. 9. Samples of the circulating fluid were collected periodically at the production and injection wellheads and from the makeup system. Injection and production conditions during the test are listed in Table VIII. Figures 10 and 11 show the concentration-time history of dissolved SiO_2 and chloride in the fluid produced at GT-2B.

Samples taken early in the test have high concentrations of dissolved species (TDS$\sim$3300 ppm) and probably represent undiluted fluid contained in the reservoir several months prior to this experiment. Relatively fresh makeup water ($\sim$ 400 ppm TDS) is injected into the reservoir where it mixes with and dilutes the fluid contained in the fracture system. Initially, when the makeup water rate is high, the dilution effect dominates and concentrations are low as shown by the TDS levels listed in Table VIII. As recirculation continues and the water loss rate to permeation decreases

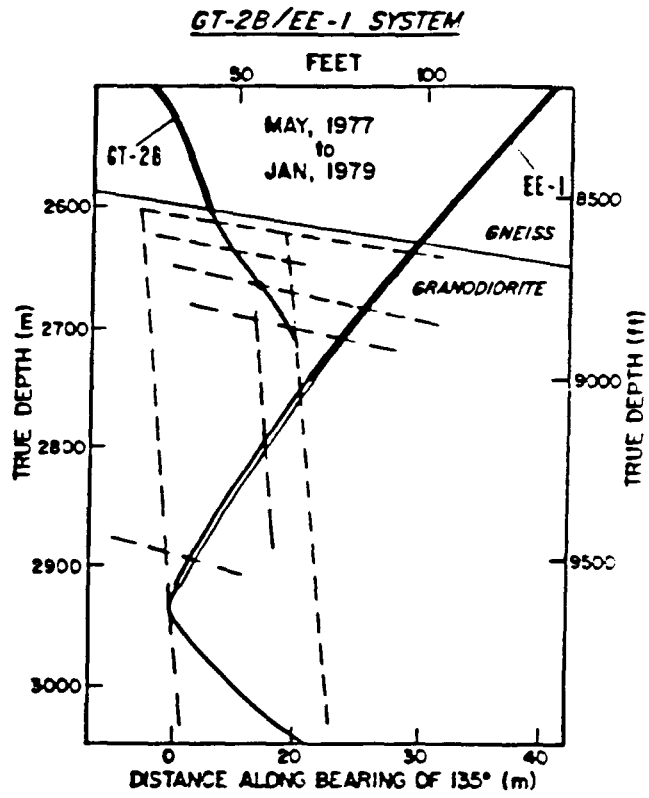

Fig. 9 - Elevation View of the EE-1/GT-2B Wellbore and Fracture System. Note that the horizontal scale is exaggerated by a factor of ten over the vertical scale. Vertical fractures and connecting 60° joints are depicted by dotted lines.

Table VIII - 75-Day Operating Conditions EE-1/GT-2B
Fenton Hill System

	Initial	Final
Injection Pressure (EE-1)	90 bar	55 bar
Production Pressure (GT-2B)	12 bar	12 bar
Buoyancy-ΔP Effect	18 bar	8 bar
Injection Flow Rate	7.9 kg/s	14.5 kg/s
Power Produced	2 MW(t)	5 MW(t)
Average Reservoir Temperature	174°C	95°C
Flow Impedance	15 bar-s/liter	3 bar-s/liter
Effective Heat Transfer Area	8000 m^2	8000 m^2
Water Loss Rate	>3 liter/s	<0.02 liter/s
Fluid Mixing Index*	0.6	1.1
Total Dissolved Solids (TDS)	540 ppm	2000 ppm

*Expressed as inverse dispersive Peclet number (see ref (2), section 4.2).

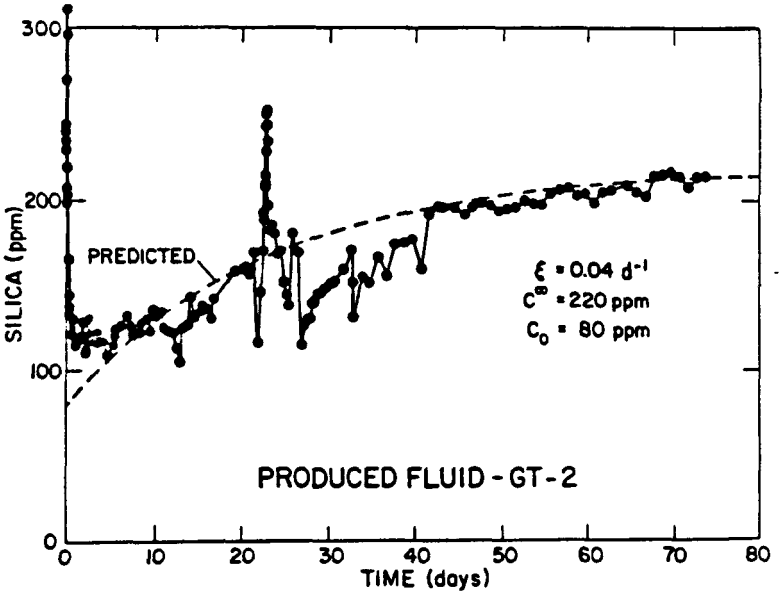

Fig. 10 - Dissolved SiO_2 Concentration History During the 75 Day Phase 1 Test. Theoretical fit shown as dotted line with $\xi = 0.04\ d^{-1}$.

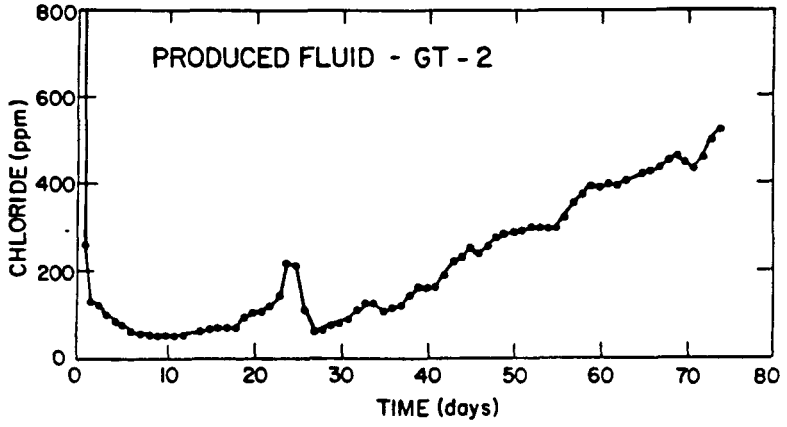

Fig. 11 - Dissolved Chloride Concentration History During the 75 Day Phase 1 Test.

(see Fig. 12), the concentration of dissolved material rises and eventually approaches an asymptote. Local fluctuations in concentrations can be explained by perturbations in loop operation. For example the sharp peak on day 23 corresponds to a sudden change in flow impedance, a short shut-down and a resulting partial flow back of fluid (see Fig. 12). Water which had been forced into the rock pores returned to the circulating system because of a transitory pressure decline, providing a source of high concentration fluid. As the system returned to its initial injection pressure, the fluid again diffused into the formation and short-duration, high makeup flows were required. Assuming the system is limited by quartz-controlled silica saturation, the asymptotic value of SiO_2 concentration shown in Fig. 10 suggests a reservoir temperature of 188 ℃. However, within three days after start up, the downhole measured temperature was below 160 ℃ corresponding to a quartz-controlled saturation concentration of less than 147 ppm. Clearly the declining mean reservoir temperature could not account for the increasing SiO_2 content in the fluid. A secondary flow path at the initial reservoir temperature or higher is required. This agrees with interpretations based on the Na-Ca-K thermometer. Temperature-flow measurements suggest that secondary flow occurs in a lower fracture system leaving EE-1 at ≈2940 m as shown in Fig. 9. If we assume that this region remains isothermal throughout the 75-day period and that active dissolution of quartz occurs within this region and that no dissolution or reprecipitation occurs in the cooler main flow path, a differential material balance shows that the rate of accumulation of SiO_2 results from a superposition of three principle effects: fluid loss due to permeation, makeup of permeated fluid, and the production of SiO_2 due to active dissolution and/or displacement in the hot region. Because the total circulation time is large compared to the overall mean residence time, τ, the material balance is written as (4)

$$V\frac{d\bar{C}}{dt} = \dot{q}_1(C_{in} - \bar{C}) + \dot{q}_2\,(1 - e^{-ka^*\,\tau_f})\,(C^{\infty} - C_{in}) \qquad (4)$$

where

$$C_{in} = \left[\frac{\dot{q}_t - \dot{q}_{loss}}{\dot{q}_T}\right]\bar{C} + \left[\frac{\dot{q}_{loss}}{\dot{q}_T}\right] C_m$$

V = total volume of primary and secondary flow paths = V_1+V_2

C_m = (SiO_2) makeup = SiO_2 concentration in the makeup water = 80 ppm

C^∞ = $(SiO_2^{sat})_{T=Tmax}$ = quartz controlled saturation concentration of SiO_2 at T_{max}

$\bar{C}$ = $(\overline{SiO_2})$ = average concentration of SiO_2 at time t

k = dissolution mass transfer coefficient, cm/sec

a^* = ratio of interfacial area to fluid volume, cm^2/cm^3

$\dot{q}_2$ = fluid circulation rate through hot region at time t

$\dot{q}_{loss}$ = $\dot{q}_{makeup}$ = fluid loss rate to permeation at time t

τ_2 = mean residence time in hot region (secondary flow path)

f = fraction of plug flow conversion = function of dispersion in hot region ($0 \leq f \leq 1$)

In the case of low water loss and rapid reaction in the hot region ($ka^*\tau_2 f >> 1$), eq.(1) reduces to

$$\bar{C} = C^\infty - (C^\infty - C_o)e^{-\dot{q}_2 t/V} = C^\infty - (C^\infty - C_o)e^{-\xi t} \qquad (5)$$

The solution to this equation with $\xi = 4.63 \times 10^{-7}$ sec^{-1}, (0.04 d^{-1}),

$C^\infty = SiO_2^{sat}{}_{T=180°C}$ = 220 ppm SiO_2 and $C_o = SiO_{2\,initial}$ (t=0) = 80 ppm

(the SiO_2 concentration of the makeup water) is shown as the dotted line on the SiO_2 plot of Fig. 10. Rate equations of the same form were applied to the fluoride, sulfate and the $^{87}/^{86}Sr$ data with the same success. Remarkably, the value of ξ is in each case $4.63 \times 10^{-7} sec^{-1}$. Since in all probability more than one mineral is dissolving to contribute SiO_2, $SO_4^=$, F^- and Sr^{+2} to the solution, it would be quite remarkable if all dissolution rates are equal. A more plausible mechanism is suggested by the solution to the material balance equation (4). The value of 4.63×10^{-7} sec^{-1} for the time constant ξ also appears reasonable if about 1 to 2% of the flow leaves EE-1 at ~2940 m and enters the lower fractured region before returning to GT-2B. Fluid residence time distribution studies conducted during the 75-day test suggest that the volume of this secondary flow path could be as large as 200,000 ℓ with a production flow rate of ~0.22 ℓ/s. This yields an estimate of ξ of 11.0×10^{-7} sec^{-1} which compares quite well with the empirical value of 4.63×10^{-7} sec^{-1} considering the uncertain knowledge of the flow geometry and in situ reaction kinetics.

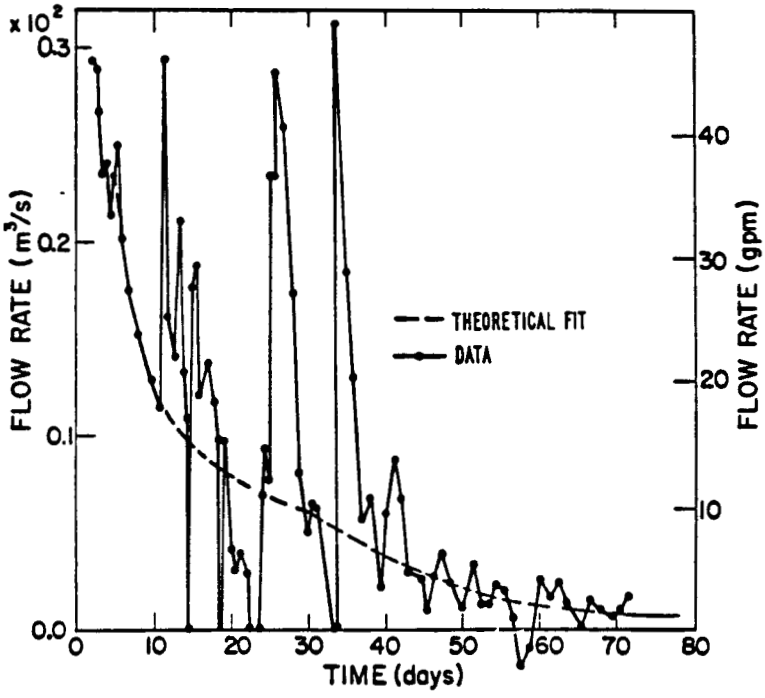

Fig. 12 - Water Loss Rate During the 75 Day Phase 1 Test. Fluctuations in rate are caused by unscheduled shutdowns and startups of the circulation loop. The general decreasing trend in loss rate is adequately described by a one-dimensional transient diffusion model accounting for permeation perpendicular to the fracture surface into the formation.

For example, if the secondary flow rate is somewhat higher and the volume smaller, similar fits to the data would result if saturation was not reached in the secondary path, that is $ka^*\tau_i f < 2$.

As seen in Fig. 11 chloride concentrations also show a marked increase with time, possibly indicating displacement and/or mixing with saturated pore fluid because no solid mineral source of chloride is known to exist at the reservoir conditions.

Conclusions

Geothermometry

Our experiments point out the limitations of the silica geothermometer. This thermometer will not yield rigorously correct temperatures because the system is not completely saturated with respect to quartz. Other reactions involving silica (i.e. producing phillipsite and possibly

laumontite) lower silica activity from the pure quartz - water system. While the assumption of quartz saturation is a good approximation at low temperatures (<100°C), the silica concentration deviates from quartz saturation more noticeably at high temperatures in multicomponent systems. The distilled water/granite system is about 30°C low at a nominal temperature of 200°C. The actual HDR reservoir natural system is not this far off due to the presence of other ions in the solution, principally carbonate. These observations are in agreement with the work of Khitarov(9). We emphasize that these observations do not entirely negate the use of the silica geothermometer. It must be modified at higher temperatures to take into account other equilibria.

On the other hand, the Na-Ca-K geothermometer apparently involves equilbration of a solution with secondary phases growing principally on the feldspars. Experience here and with the geothermal well indicates the Na-Ca-K geothermometer also "remembers" the highest temperatures more readily. The Na-Ca-K solutions metastably persist at higher temperature equilibrium values while the silica begins to re-equilibrate toward the lower temperature concentration. Currently, experiments are underway to determine which phases and reactions control the Na-Ca-K geothermometer.

Mineral Solubility

Precise determination of the solubility of amorphous silica is difficult because it is thermodynamically unstable in the regions it is being studied. Crystallization of silica to other polymorphs yields lower values for amorphous silica concentration.

Alkaline solutions rapidly leach silica from the reservoir rock. However, field tests show that large amount of alkali solutions are required to significantly increase the matrix permeability.

All solubility studies depend upon the method of sample preparation. If care is not taken to reduce the very high surface free energy of the starting material for the experimental system, apparent supersaturation results. This observation has some application in field experiments when new fractures are opened by hydrofracture.

Wall Rock Alteration

The experiments show that early in reservoir life reactivity is controlled by the presence of quartz which suppresses the solubility of the other mineral phases. Should most of the quartz be removed and deposited elsewhere in the system, reactivity will be controlled by feldspar dissolution. The principal secondary phase early in the reservoir life appear to be zeolites which should not interfere with reservoir operation.

Movement of silica down the temperature gradient (6) may explain higher impedance in the downhole system after shutin for a period of months. This effect has been observed in another circulation system which had a controlled temperature gradient. With a gradient of 50 to 310°C across the vessel (91.5 cm or 36 in. long), silica did deposit in the cool end of the vessel. For the field system, the situation is more complicated because geochemical, pore pressurization, and thermal stress effects are superimposed.

The natural fluids contain Cl^-, $SO_4^=$, and $CO_3^=$. These ions are not in sufficient concentration to suppress the appearance of zeolites. At higher

P_{CO_2}, zeolites will be suppressed in favor of carbonate phases. Currently, experiments have begun reacting granodiorite with a mild (0.01 N) Sodium chloride solution to test effects of other ions.

Experimental secondary phases consisted of discrete overgrowths and did not appear to form a continuous layer of precipitate as envisioned by Correns and Von Engelhard(4) and Helgeson(6). Reactions to form secondary phases appear to be fixed by reaction of fresh rock with solution. Primary phases can act as a template for nucleation of secondary phases with similar structure, for example, phillipsite on plagioclase. Both phases are framework silicates.

Concerning the reservoir rock, the host biotite granodiorite has a high temperature mineral assemblage, and shows clear signatures of at least two metamorphic events: First, epidote - prehnite - quartz characteristic of very low to low grade metamorphism at about 250 ± 50°C, and second, very low grade metamorphism at higher P_{CO_2} producing calcite + quartz veining at about 200°C. The host rock is better equilibrated with the first (older) signature and is well out of equilibrium with the second. After the proposed deepening of the well is completed the host rock at the new depth would be expected to be more in equilibrium with ambient conditions.

Field Experiments and Modeling

The geochemical behavior during a long-term circulation test in a fractured, granodiorite reservoir was adequately described by a differential material balance which accounts for fluid mixing and chemical dissolution within different regions of the reservoir.

Acknowledgments

The authors gratefully acknowledge the technical assistance provided by J. Abbott, D. Counce, R. Vidale, and C. Duffy. The help of the Geothermal Operations Group (G-4) in implementing the field tests are greatly appreciated. The authors are greatly indebted to B. Hahn, B. Ramsay, and M. Jones for the careful preparation of this manuscript.

References

1. M. C. Brown, R. B. Duffield, C. L. B. Siciliano, and M. C. Smith, "Hot Dry Rock Geothermal Energy Development Program," Annual report FY 1978, Los Alamos National Laboratory report LA-7807-HDR, April, 1979.

2. R. W. Charles, "Experimental Geothermal Loop: I, 295°C Study," Los Alamos National Laboratory report LA-7334-MS, July, 1978.

3. R. W. Charles, "Experimental Geothermal Loop: II, 200°C Study," Los Alamos National Laboratory report LA-7735-MS, April, 1979.

4. C. W. Correns and W. Von Engelhard, "Neue Untersuchungen Uber Die Verwitterung Des Kalifelspates," Chem. Erde. 12, p. 1-22 (1938).

5. R. O. Fournier and A. H. Truesdell, "Chemical Indicators of Subsurface Temperature. Part 2: Estimation of Temperature and Fraction of Hot Water Mixed with Cold Water," J. Res. U.S. Geol. Surv., 2, p. 263-270 (1974).

6. R. O. Fournier, Private Communication, U.S. Geol. Surv., October, 1979.

7. H. C. Helgeson, "Chemical Interaction of Feldspar and Aqueous Solutions," p. 184-217 in The Feldspars, W. S. McKenzie and J. Zussman, eds., Manchester University Press (1972).

8. J. V. Walker and H. C. Helgeson, "Calculation of the Thermodynamic Properties of Aqueous Silica and the Solubility of Quartz and its Polymorphs at High Pressures and Temperature," Am. J. Sci., 277, p. 1315-1351 (1977).

9. N. I. Khitarov, "The Chemical Properties of Solutions Arising as a Result of the Interaction of Water with Rocks at Elevated Temperature and Pressure," Geochem. Int., 6, p. 566-578 (1957).

10. G. W. Morey, R. O. Fournier, and J. J. Rowe, "The Solubility of Quartz in Water in the Temperature Interval from 25°C to 300°C," Geochim. Cosmochim. Acta, 26, p. 1029-1043 (1962).

11. R. A. Robie, P. M. Bethke, and K. M. Beardsley, "Selected X-ray Crystallographic Data, Molar Volumes, and Densities of Minerals and Related Substances," GSA Bull. 1248 (1967).

12. M. C. Smith, R. L. Aamodt, R. M. Potter, and D. W. Brown, "Man-made Geothermal Reservoirs," in 2nd United Nations Geothermal Energy Symp., San Francisco, California, May 20-29, 1975, p. 1781-1787 (United Nations, 1975).

13. J. W. Tester and M. C. Smith, "Energy Extraction Characteristics of Hot Dry Rock Geothermal Systems," Proc. 12th Intersociety Energy Conversion Engineering Conf., Washington, D.C., August 28-September 2, 1977 (American Nuclear Society, 1977), p. 816.

14. J. W. Tester and J. N. Albright, Eds., "Hot Dry Rock Energy Extraction Field Test: 75 Days of Operation of a Prototype Reservoir at Fenton Hill," Los Alamos National Laboratory report LA-7771-MS, April 1979.